Rev. Roum. Sci. Techn.– Électrotechn. et Énerg.
Vol. **65**, *1-2*, pp. 97–102, Bucarest, 2020

COGNITIVE WIDEBAND SENSING USING CORRELATION OF INVERTED SPECTRUM SEGMENTS

ASHWINI KUMAR VARMA, DEBJANI MITRA

Key words: Cognitive radio, Wideband spectrum sensing, Variable noise floor, NI-USRP 2942R.

Cognitive radio (CR) is one of the forthcoming technologies for efficient spectrum utilization. It is critically dependent on fast and accurate spectrum sensing which becomes challenging for wideband systems that typically suffer from low and variable signal to noise ratio (SNR) conditions. For wideband sensing, simple energy detection is usually augmented by the double threshold method using forward consecutive mean excision (DT-FCME) algorithm, or approached by eigenvalue detection (EVD). For both these methods, it is difficult to get both high accuracy and fast sensing at same time. In this paper, an algorithm named as correlation of inverted spectrum segments (CISS) is proposed which computes in a specific manner, the cross-correlation of intra sets of successive sub-bands in the spectrum of wideband sensing data. The approach is significantly faster than both EVD and DT-FCME and maintains high detection probability. In addition, the detection performance under low and variable SNR is also better than the conventional methods used in wideband sensing. The algorithm is analyzed mathematically, and applied to synthetic and real time GSM data captured from an universal software radio peripheral (USRP) setup. The algorithm would be useful as a robust and fast sensing scheme for wideband CR system.

1. INTRODUCTION

The challenge of handling proliferation of wireless devices under severe scarcity and underutilization of spectrum can be mitigated by cognitive radio (CR) devices enabled with the functionality of spectrum sensing [1, 2]. The next-generation communication network will require sensing a wide range of frequencies without much information about the type of signal present. In most of the sensing algorithms there exists a trade-off between sensing time, detection performance and complexity, which is difficult to be obtained. The waveform based sensing techniques of cyclostationary and matched filtering, are fast and reliable but require prior knowledge of features of primary user signal (such as type of modulation, symbol rate, cyclic frequencies, etc.) which are not always available to CR users [3]. Conventional energy detection (ED) does not require any signal information but degrades in performance over wideband sensing due to low SNR regimes, unknown noise statistics and rapidly changing environment of noise and interference [4]. Eigenvalue based detection (EVD) and its variants are advanced in providing superior performance under noise uncertainty [5]. The sensing decision is based on eigenvalues of covariance matrix of received signal samples. EVD is traditionally used for wideband sensing but is characterized by high computational complexity involving calculating the covariance matrix and its decompositions for eigenvalues. Besides, sensing in a wideband the poses difficulties of analog to digital converter (ADC) implementation with increased sampling rate, leading to higher complexity and sensing time. Advanced spectral techniques such as compressed sensing using sub-Nyquist sampling can be applied to the received signal to lower the required sampling rates [6]. However, it requires a high level of sparsity of received signal for reconstruction. The other approach of wideband sensing is through power-spectrum segmentation and estimation of boundaries and/or spectral energy in each of the sub-bands that are usually fixed and known [7]. In multi-taper method, the periodogram of each windowed segment is averaged both along consecutive segments and orthogonal tapers within each segment [8]. Wavelets can detect local spectral edges and relate them to frequency location of the channels, but they also are computationally intensive [9]. In this paper we propose a new algorithm that is computationally simpler, yet accurate for wideband sensing. In Section 2, the background of related works towards the motivation is discussed. The next two sections describe the proposed CISS algorithm, its analysis, performance, complexity and results of application to data captured from an experimental setup. The overall merits and significance of the results are summarized in the last section.

2. MOTIVATION AND RELATED WORK

The challenge of obtaining both a good accuracy and a short sensing time remains a major technical challenge to be addressed in developing a computationally simple wideband sensing method, which is the main motivation for the current work. With increased efficiency of spectrum usage by CR networking in future, signals are expected to occupy several sub-bands in a wideband spectrum. Compressed Sensing may therefore fail due to non-sparsity. Besides, the wide band under variable noise floor, may lead to low SNR and noise uncertainty, under which compressed sensing will be unsuccessful. On the other hand, the simple approach of ED to ascertain power spectral density in each sub-band can be made accurate and robust against noise uncertainty by using an adaptive decision threshold. The Double Threshold method using forward consecutive mean excision (DT-FCME) detection uses a threshold dependent on mean of sample energy and a parameter extracted from the statistical properties of noise that is assumed to be Gaussian [10]. The noise parameter is set using a constant false alarm rate. The performance of the method is sensitive to the number of samples, noise properties and the pre-set value of the false alarm probability but works well in narrowband sensing. ED is optimal for independent identically distributed (i.i.d) signals, but in most practical systems, signals may be correlated [5]. In [11], authors report improvement on the vulnerability to noise uncertainty by use of energy and autocorrelation statistics. EVD is robust against noise variability but relies on the estimation of autocorrelation of successive samples of received signal, and deviation of the sample covariance matrix from the statistical one seriously affects the performance [5]. As reported in [12], segmentation and decimation of the digitized

Indian Institute of Technology (Indian School of Mines), Department of Electronics Engineering, Dhanbad, India
E-mail: akvarma.iitism@gmail.com

samples is able to detect the energy of the signal effectively with almost one tenth of the complexity of the simplest correlation based technique. Weijia Han *et al.* [13] have used oversampling to explore the intra symbol correlation in amplitude and phase pattern of the transmitted signal. The algorithm significantly improves the sensing performance compared to several existing sensing schemes. Several other recent works on realistic sensing in practical CR systems prefer the use of second order statistic of correlation information derived from received signal samples [14–16]. However, most of the existing related works deal with narrow band sensing and consider correlation in time domain.

This paper investigates sample correlation under simple wideband ED in frequency domain, which to the best of our knowledge has not been commonly reported. The EVD approach of course is equivalent to Fourier transformation over the empirical covariance function, for which complexity and therefore speed is a major limitation to overcome. Our proposed algorithm named as correlation of inverted spectrum segments (CISS) computes the cross-correlation of two parts of each spectrum sub-band where the sequence of one of the part is inverted. This helps to effectively distinguish noise and signal samples in the sub-band. The approach has relatively lower complexity and is significantly faster than both the EVD and DT-FCME. The detection performance under low and variable SNR is also better than conventional methods used in wideband sensing. The CISS approach can thus be a simpler alternative to wavelet based detection and compressed sensing (CS) for wideband detection. On practical CR platforms, CS is usually too complex while wavelets are incapable of detecting edges when received power from occupied sub-band is low. The CISS algorithm overcomes both the limitations with reasonably good performance accuracy. It is tested over real time 25 MHz GSM band data using NI-USRP 2942 experimental setup. We also quantify the probabilities of detection and false alarm through numerical simulations and support the same through theoretical validations.

3. THE PROPOSED ALGORITHM

Any energy detection type of sensing scheme is formed around a hypothesis testing problem to detect the presence or absence of primary user (PU)

$$\begin{aligned} H_0 &: R(k) = W(k), \\ H_1 &: R(k) = S(k) + W(k), \end{aligned} \tag{1}$$

where $S(k)$ is the signal of interest while $W(k)$ represent the background noise. The decision of hypothesis test H_0 (PU signal absent) and H_1 (PU signal present) is conventionally computed using $R(k)$ directly as the energy value. Also, a fixed threshold derived from a constant false alarm rate is assumed. The approach is unsuitable because single binary decision for the whole spectrum may not be capable of identifying individual spectral opportunities that lie within the wideband spectrum. In our algorithm, we therefore propose to divide the entire bandwidth into sub-bands and extract an appropriate threshold that takes care of the variable noise floor. The decision statistic $R(k)$ in our case is what we call CISS values computed for successive sub-bands which is compared with the threshold for knowing the presence or absence of PU signal. All computations are in frequency domain representation of the received samples. Sub-bands are created using rectangular windowing of length l. Each sub-band is divided into two parts as arrays V_a and V_b. The cross correlation value of the inverted sequence of V_a with V_b is derived as a new data array, *R*, which is compared with a pre-defined threshold for sensing decision of signal presence. The threshold *T* that is used to detect the presence of PU is carefully selected as [17]

$$T \geq 3\sigma_R = \frac{3\sigma_n}{\xi l^{\vartheta}}. \tag{2}$$

where σ_R and σ_n represent the standard deviation of CISS values and noise respectively, while the two parameters ϑ and ξ are defined as $\vartheta \approx 1$ and $\xi >> \vartheta$. However, the proposed scheme is outlined through the following algorithmic steps:

Algorithm 1: CISS Model

1. Initialize l (Rectangular Window Length)
2. $X \leftarrow$ Sensed data in Frequency domain
3. $L \leftarrow length(X)$
4. Initialize $k \leftarrow 1$
5. $m \leftarrow k$
6. **repeat**
7. for $i \leftarrow 1$ to $l/2$
8. do
9. $V_a[i] \leftarrow X[k]; \quad k \leftarrow k+1;$
10. for $i \leftarrow 1$ to $l/2$
11. do
12. $V_b[i] \leftarrow X[k]; \quad k \leftarrow k+1;$
13. $j \leftarrow 1$
14. for $i \leftarrow l/2$ to 1
15. do
16. $V_a'[i] \leftarrow V_a[j]; \quad j \leftarrow j+1;$
17. ▷ $V_a' \leftarrow$ Inverted sequence of V_a
18. $R[k] \leftarrow cross\_correlation(V_a', V_b); m \leftarrow m+1; k \leftarrow m;$
19. **until** $k \leq L-(l-1)$
20. ▷ return statistical decision variable $R[k]$
21. Compute Threshold '*T*'
22. for $k \leftarrow 1$ to $L-(l-1)$
23. do
24. if $R[k] > T$
25. then
26. for $m \leftarrow k$ to $k+l$
27. do
28. $Y[m] \leftarrow 1$
29. ▷ where, 1 represent H_1 hypothesis
30. $k = k+l$
31. else if $R[k] < T$
32. then
33. $Y[k] \leftarrow 0$
34. ▷ where, 0 represent H_0 hypothesis

The correlation is computed between two parts of the sub-band samples where one part is inverted with respect to the sample sequences. The benefit of inverting is illustrated through Fig. 1 and Table 1. A signal in the range 810 MHz to 812 MHz (Fig. 1(a)) was subjected to the algorithm. The correlation value of the corresponding vectors V_a and V_b (of length 450 samples) was computed both with and without inversion as shown in Table 1. The inverted sequence of V_a (*i.e.* the last sample is made the first sample, the second last sample become the second sample and so on) when correlated with V_b gives a highly distinguishable spike as shown in Fig. 1(b). The spike value can be compared to the threshold for the decision of signal presence or absence. Unlike the conventional wideband ED methods, our approach is seen to be robust against low SNR and noise uncertainty. This is because irrespective of noise floor, the correlation values of the inverted segment with the successive segment will always be high whenever signal samples are present within a frequency range. When PU signal is absent, for the corresponding sub-band, the correlation of inverted V_a and V_b will always be near to zero as shown in Table 1. The simple operation of inversion before correlation has the capability to differentiate between a low SNR and noise signal. Thus, this technique can effectively make distinction between signal and noise over a wideband without the requirement of complex computations of wavelet detection and compressed sensing. Unlike the FCME algorithm, the performance of our algorithm will not degrade at low SNR and can incorporate the effects of noise floor variation.

Table 1
Effect of inversion on correlation values

Signal Type	Correlation of V_a and V_b	Correlation of inverse V_a and V_b
Low SNR Signal (–10 dB)	–0.3193	0.7752
High SNR Signal (+20 dB)	–0.3521	0.9372
Additive white Gaussian noise (AWGN)	0.0189	–0. 0281

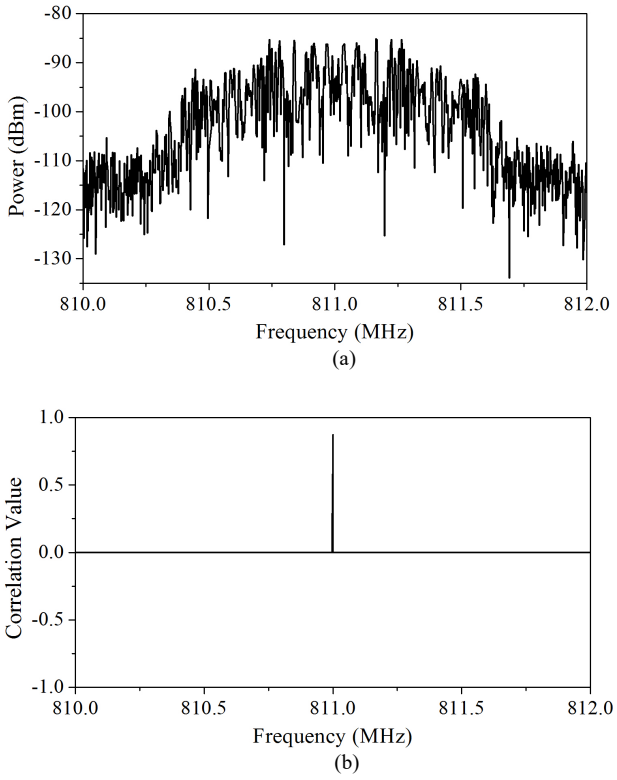

Fig. 1 – a) Test signal, b) Output of CISS.

The successive sub-bands are formed as below by sliding the window over the sequence of spectrum segments:

$$x_1, x_2, x_3, x_4, \ldots\ldots, x_l, x_{l+1}, x_{l+2}, x_{l+3}, \ldots\ldots, x_L$$

First sub-band : $x_1, x_2, x_3, \ldots\ldots, x_l$
Second sub-band : $x_2, x_3, x_4, \ldots\ldots, x_{l+1}$
Third sub-band : $x_3, x_4, x_5, \ldots\ldots, x_{l+2}$.

The decision variable R in the algorithm represents the correlation coefficient which is a random variable bounded between [0, 1] in magnitude. For wideband sensing, in the vicinity of the signal region, the value will be close to one while in the noise region it will be close to zero. Therefore $f(r)$, the probability density function of R can be assumed as normal distribution under H_0 and beta distribution under H_1. Hence,

$$f(r) = \begin{cases} \dfrac{1}{\sigma\sqrt{2\pi}} e^{-\frac{(r-\mu)^2}{2\sigma^2}} & ,H_0 \\ \dfrac{\Gamma(\alpha+\beta)}{\Gamma(\alpha)\Gamma(\beta)} r^{\alpha-1}(1-r)^{\beta-1} & ,H_1, \end{cases} \quad (3)$$

where α and β represent the shape parameters of beta distribution and $\Gamma(.)$ is the gamma function. With R as the decision variable, there are two type of possible errors: (i) when the model decides H_1 but H_0 is correct: $P(H_1|H_0)$, probability of false alarm (P_{FA}) and (ii) when the model decides H_0 while H_1 is true: $P(H_0|H_1)$, probability of miss detection (P_{MD}). Complementary of P_{MD} is probability of detection (P_D). For the proposed mode these performance measures are defined as:

i) Probability of false alarm (P_{FA})

Based on distribution of R under H_0, P_{FA} can be evaluated as

$$\begin{aligned} P_{FA} &= P(H_1|H_0) = P(r > T; H_0), \\ &= \int_T^1 f(r)\,\mathrm{d}r \qquad ,H_0 \\ &= \frac{1}{2}\left[\operatorname{erf}\left(\frac{1-\mu}{\sigma\sqrt{2}}\right) - \operatorname{erf}\left(\frac{T-\mu}{\sigma\sqrt{2}}\right) \right], \end{aligned} \quad (4)$$

where $\operatorname{erf}()$ is the error function [17].

ii) Probability of detection (P_D)

Using beta distributed under H_1, P_D can be expressed as

$$P_D = P(H_1|H_1) = P(r > T; H_1)$$

$$= \int_{T}^{1} f(r)\,\mathrm{d}r \qquad , H_1 \tag{5}$$
$$= 1 - \frac{B(r;\alpha,\beta)}{B(\alpha,\beta)} = 1 - \mathrm{I}_r(\alpha,\beta).$$

where $\mathrm{B}(,)$ represent beta function while $I_r(\,,\,)$ stand for normalized beta function or regularized incomplete beta function [18]. The intermediate steps of the derivation can be obtained by referring [19].

3.1 SMOOTHED CISS (SCISS)

It is observed that in wideband sensing, the signal power measurements are extremely slow changing variables due to which the proposed CISS approach makes too many redundant computations that slow down the sensing process. To overcome this problem the total number of sensed L samples were divided into S sub-bands, each of width P % of L and mean was taken over $m = L / S$ number of samples in each sub-band. Therefore, the outcome in the form of smoothed array has now only S samples to process. Under such circumstances the detection threshold, T is reframed and is defined as [17]:

$$T \geq 3(m+1)\sigma_R = \frac{3(m+1)\sigma_n}{\xi\, l^{\,\vartheta}}. \tag{6}$$

As a result, the process of applying smoothing before performing CISS reduces the number of samples to be processed which ultimately reduce the computation time of the algorithm significantly. This smoothening effect would also depend on the width of the sub-band controlled by the parameter P.

4. EXPERIMENTAL SETUP AND RESULTS

Noise uncertainty and low SNR affects accuracy of most wideband spectrum sensing (WSS) techniques. For example, in Fig. 2 our simulation of detection performance for multi-channel DFT filter bank sensing shows a strong degradation of probability of detection, P_D below SNR of -10 dB under increasing noise variance σ_n^2. This is due to the use of static noise dependent threshold $\left(\mathrm{Q}^{-1}(P_{fa})\sqrt{\overline{N}} + \overline{N}\right)\sigma_n^2$ as discussed in [20]. The plots use probability of false alarm, $P_{FA} = 0.10$ and the number of samples per channel $\overline{N} = 1500$.

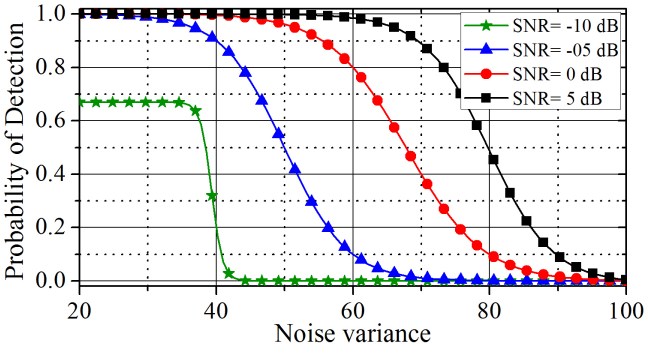

Fig. 2 – P_d *vs.* noise variance plot for filter bank sensing technique.

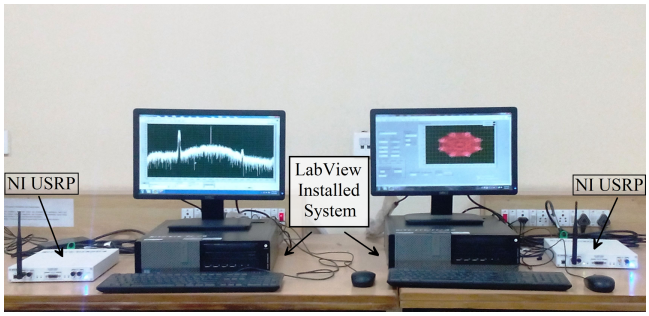

Fig. 3 – The experimental setup.

Through the proposed CISS algorithm we avoid the use of noise dependent detection threshold hence increases it performance over real-time signals. Figure 3 shows the experimental setup using a pair of NI-USRP 2942R interfaced through LabView software. Two QPSK signals with variable SNR and a fix bandwidth of 400 kHz were generated at 815 MHz and 825 MHz under variable noise floor condition. Thereafter, a band of 20 MHz (810–830 MHz) within which the two signals were generated was sensed with acquisition time of 500 µs. The acquired power spectrum data was further given to the proposed algorithm to test its effectiveness over real-world spectrum data. Figures 4 and 5 show respectively the detection performance of this signal pair using DT-FCME and CISS algorithm. The low SNR signal at 825 MHz is miss-detected by the conventional DT-FCME approach, while the robustness of the CISS algorithm is clearly demonstrated through the figure. The algorithm performs equally well at both low and high SNR regimes. This is because of the inversion technique. This ensures that signal samples will always show correlation close to one while the noise samples will show correlation value near to zero.

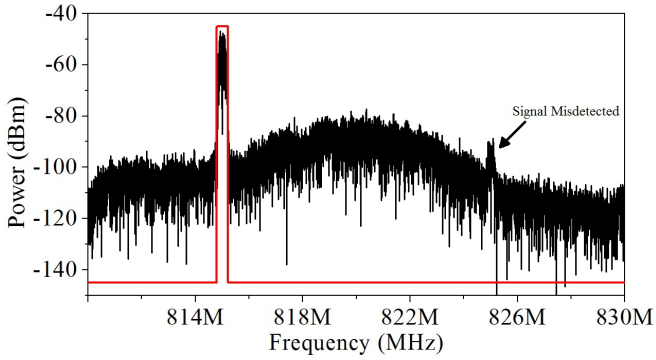

Fig. 4 – Low SNR signal miss-detected by DT-FCME technique.

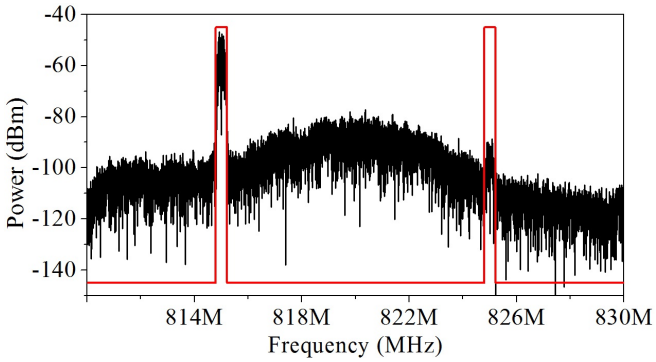

Fig. 5 – Both the signals are detected accurately using CISS algorithm.

Under the assumption of equation (3), the correlation values of the signal sensed through NI-USRP obtained

through CISS were fitted to beta distribution with $\alpha = 9.6679$ and $\beta = 2.3745$. The variable noise floor was characterized by $\mu = -0.0118$ and $\sigma^2 = 0.0183$ variance. The suitability of the CISS for a wide range of variable noise floor is shown through the receiver operating characteristic (ROC) curve (P_D *vs.* P_{FA}) in Fig. 6. It also shows that the proposed model outperforms the conventional EVD method.

We have also compared the performance of the CISS detector with eigenvalue detection (EVD) and DT-FCME in terms of complexity, computational time and accuracy of detection as shown in Table 2. Significant improvement of both is clearly established. The smoothening operation has a strong impact on the speed of the algorithm. The effect of P has been evaluated in the table. The pre-processing step of taking mean is an essential step to reduce the computational time without compromising much on the detection accuracy. To evaluate and compare the performance of CISS and smoothed CISS with different value of P, a simulation model is build. In simulation, BPSK modulated signal with square root cosine pulse of 0.22 roll-off factor was generated over a wide range of spectrum and was sensed using the proposed algorithm. Figure 7 shows the detection probability as a function of wide range of low SNR plot obtained using CISS and smoothed CISS. The figure shows the effect of smoothing parameter, P which plays an important role. From the figure one can clear observe the deterioration of detection probability with increased value of P. However, from the results of the proposed CISS and Smoothed CISS technique as shown in Fig. 7 and Table 2 one can conclude that Smoothed CISS with P as 0.05 is an efficient wideband sensing technique without prolonging sensing time or increasing hardware complexity.

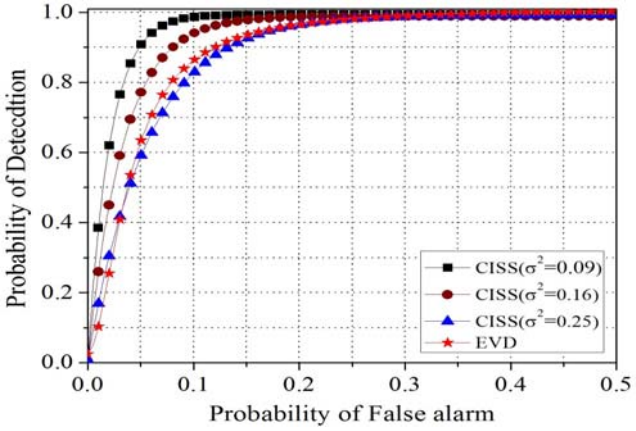

Fig. 6 – P_D *vs.* P_{FA} plot with different values of σ^2 and EVD method.

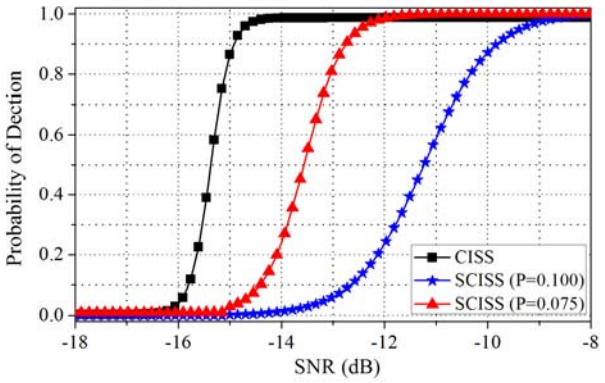

Fig. 7 – Probability of detection Vs SNR for CISS and smoothed CISS with different value of P.

Real-time 25 MHz GSM spectrum data (both uplink channel: 890–915 MHz and downlink channel: 935–960 MHz) is subjected to the CISS for detection as shown through Fig. 8(a) and 8(b). The robustness of the algorithm about noise uncertainty is prominently visible in downlink channel.

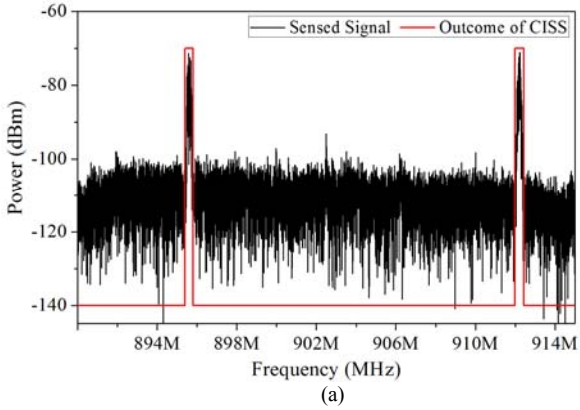

(a)

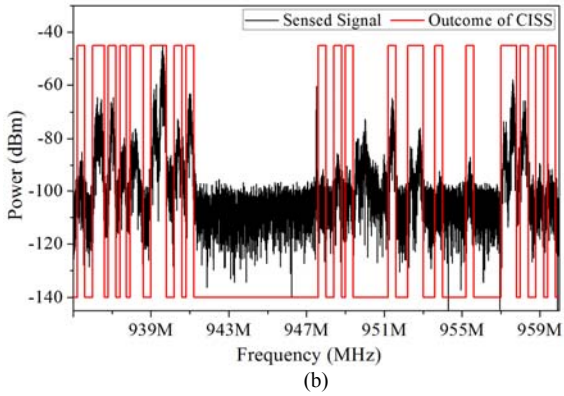

(b)

Fig. 8 – Real time wideband spectrum sensing of (a) GSM uplink channel (890–915 MHz), (b) GSM downlink channel (935–960 MHz).

Table 2
Computational time* and accuracy comparison

Methods		Complexity (in big O form)	Computational time (in s)	Accuracy (in percentage)
DT-FCME based detection		$O(L^2)+O(L)$	6.8508	62
EVD based detection		$O(L^3)+O(L)$	3.3269	90
CISS based detection (with smoothening)	$P = 0.050$	$O((L/(P\%*L))*(P\%*L)) + O((L/(P\%*L))*3l) + O(L/(P\%*L))$	0.6982	95
	$P = 0.075$		0.4639	
CISS based detection (without smoothening)		$O(L*3*(l/2))+O(L)$	11.870	98

*Computational time was measured on Intel® Core ^{TM} 2 Duo processor, clock frequency of 2.2 GHz and 4 GB of RAM.

5. CONCLUSION

This paper presents a robust, accurate and low complexity wideband spectrum sensing technique based on correlation of two successive spectrum segments where one of the segments is inverted with respect to the sequence of samples in it. Named as CISS, the approach includes a pre-processing step in which the samples are smoothened by taking mean of the samples in each sub-band. The technique is capable of detecting signal in wideband spectrum with much higher accuracy than the DT-FCME algorithm. The accuracy obtained is slightly higher than the EVD method. In terms of speed, the proposed algorithm is much faster than both the algorithms (DT-FCME and EVD). In addition, unlike many methods, the detection performance of CISS is reasonably high even under low SNR regimes and variable noise floor conditions. The algorithm tested satisfactorily over real time as well as synthetic signals.

Received on January 10, 2019

REFERENCES

1. A. Marţian, *Evaluation of Spectrum Occupancy in Urban and Rural Environments of Romania*, Rev. Roum. Sci. Techn. – Électrotechn. et Énerg., **59**, *1*, pp. 87–96, 2014.
2. C. I. Bădoi, V. Croitoru, N. Prasad, R. Prasad, *Cognitive Radio Spectrum Management – Sensing and Sharing*, Rev. Roum. Sci. Techn. – Électrotechn.et Énerg., **55**, *3*, pp. 300–309, 2010.
3. A. Ali, W. Hamouda, *Advances on Spectrum Sensing for Cognitive Radio Networks: Theory and Applications*, IEEE Communications Surveys & Tutorials, **19**, 2, pp. 1277–1304, Second quarter 2017.
4. A. Mariani, A. Giorgetti, M. Chiani, *Effects of Noise Power Estimation on Energy Detection for Cognitive Radio Applications*, IEEE Transactions on Communications, **59**, 12, pp. 3410–3420, December 2011.
5. A. Ahmed, Y. F. Hu, J. M. Noras, P. Pillai, *Spectrum sensing based on Maximum Eigenvalue approximation in cognitive radio networks*, 2015 IEEE 16th International Symposium on A World of Wireless, Mobile and Multimedia Networks (WoWMoM), Boston, MA, 2015, pp. 1–6.
6. G. P. Aswathy, K. Gopakumar, *Sub-Nyquist wideband spectrum sensing techniques for cognitive radio: A review and proposed techniques*, AEU Int J Electron Commun, **104**, pp. 44–57(2019).
7. L. De Vito, *A review of wideband spectrum sensing methods for Cognitive Radios*, 2012 IEEE International Instrumentation and Measurement Technology Conference Proceedings, Graz, 2012, pp. 2257–2262.
8. S. Haykin, *The Multitaper Method for Accurate Spectrum Sensing in Cognitive Radio Environments*, 2007 Conference Record of the Forty-First Asilomar Conference on Signals, Systems and Computers, Pacific Grove, CA, 2007, pp. 436–439.
9. Z. Tian, G. B. Giannakis, *A Wavelet Approach to Wideband Spectrum Sensing for Cognitive Radios*, 2006 1st International Conference on Cognitive Radio Oriented Wireless Networks and Communications, Mykonos Island, 2006, pp. 1–5.
10. J. Vartiainen, J. J. Lehtomaki, H. Saarnisaari, *Double-threshold based narrowband signal extraction*, 2005 IEEE 61st Vehicular Technology Conference, 2005, pp. 1288–1292.
11. L. Gonzales-Fuentes, K. Barbé, W. V. Moer, N. Björsell, *Cognitive Radios: Discriminant Analysis for Automatic Signal Detection in Measured Power Spectra*, IEEE Transactions on Instrumentation and Measurement, **62**, *12*, pp. 3351–3360 (2013).
12. S. N. A. Ahmed, P. K. Meher, A. P. Vinod, *A low-complexity spectrum sensing technique for cognitive radios based on correlation of intra-segment decimated vectors*, 2012 IEEE International Conference on Communication Systems (ICCS), Singapore, 2012, pp. 443–447.
13. W. Han, C. Huang, J. Li, Z. Li, S. Cui, *Correlation-Based Spectrum Sensing With Oversampling in Cognitive Radio*, IEEE Journal on Selected Areas in Communications, **33**, *5*, pp. 788-802 (2015).
14. Y. Zeng, Y. C. Liang, T. H. Pham, *Spectrum Sensing for OFDM Signals Using Pilot Induced Auto-Correlations*, IEEE Journal on Selected Areas in Communications, **31**, *3*, pp. 353–363 (2013).
15. M. Naraghi-Pour, T. Ikuma, *Autocorrelation-Based Spectrum Sensing for Cognitive Radios*, IEEE Transactions on Vehicular Technology, **59**, *2*, pp. 718–733 (2010).
16. J. Lunden, S. A. Kassam, V. Koivunen, *Robust Nonparametric Cyclic Correlation-Based Spectrum Sensing for Cognitive Radio*, IEEE Transactions on Signal Processing, **58**, *1*, pp. 38–52 (2010).
17. S. Koley, V. Mirza, S. Islam, D. Mitra, *Gradient-Based Real-Time Spectrum Sensing at Low SNR*, IEEE Communications Letters, **19**, *3*, pp. 391–394 (2015).
18. S. Gradshteyn, I. M. Ryzhik, *Table of Integrals, Series, and Products*, 6th ed. San Diego, CA: Academic, 2000.
19. C. Walch, *Handbook on Statistical Distributions for Experimentalists,* Internal Report SUF-PFY/96-01, 2000.
20. M. Kim, J. Takada, *Efficient multi-channel wideband spectrum sensing technique using filter bank*, IEEE 20th International Symposium on Personal, Indoor and Mobile Radio Communications, Tokyo, 2009, pp. 1014–1018.